Design and Development of a Field-Deployable Single-Molecule Detector (SMD) for the Analysis of Molecular Markers

Supporting Information

Jason M. Emory,[1,3] Zhiyong Peng,[1,3] Brandon Young,[1,3] Mateusz L. Hupert,[1,3] Arnold Rousselet,[2] Donald Patterson,[3] Brad Ellison[4] and Steven A. Soper[1,2,3 5*]

1) Department of Chemistry, Louisiana State University, 232 Choppin Hall, Baton Rouge, LA 70803
2) Department of Mechanical Engineering, Louisiana State University, 2508 P. Taylor Building, Baton Rouge, LA 70803
3) Center for BioModular Multi-Scale Systems, Louisiana State University, 8000 G.S.R.I. Rd., Bldg. 31000, Baton Rouge, LA 70803
4) Department of Physics and Astronomy, Louisiana State University, 115 Nicholson Drive, Tower Dr., Baton Rouge, LA 70803
5) Nano-Bioscience and Chemical Engineering, Ulsan National Institute of Science and Technology, Ulsan, South Korea

***** Corresponding Author,
Phone 225 578-1527
Fax 225 578-3458
Email: chope@lsu.edu

Additional Background Information on SMD Instrumentation

A number of groups have reported on field-deployable microfluidic devices that contain the support peripherals possessing a small footprint, such as the miniature thermal cycling instrument developed by Northrup *et al.*[1] or the portable, disc-based and fully automated enzyme-linked immuno-sorbent assay (ELISA) system demonstrated by Lee and coworkers.[2] While these are good examples of integrating the support peripherals into a single compact unit, the readout phases of the assay continue to be problematic due to the fact that the generation of microsystems typically demands the analysis of minute quantities of material. For example, the analysis volume of many microfluidic systems can be on the order of 1 nL, and thus, the analysis of 1 nM would require the detector to transduce the presence of 1 amol of material. If this sampling volume is reduced to 1 pL, the mass limit-of-detection must be 1 zmol or ~600 molecules for this same concentration. Clearly, efforts in reducing the footprint of the readout hardware must take into account the required low mass detection limits often associated with microfluidics.

Genomic-based Assays

Genomic-based assays can be used for the identification of pathogenic species, such as bacteria, and provide the ability for strain specific identification to evaluate possible threat levels imposed by that bacterium. Polymerase chain reactions (PCR) are typically employed in genome assays because they can improve the sensitivity by creating millions of targets to detect from a few starting copies of the genomic DNA. PCR-based schemes have demonstrated advancements over culturing and plating methods with results usually provided in several hours.[3] Examples of different PCR methods developed for bacterial detection are: (i) real-time PCR[4] (ii) multiplex PCR[5] and (iii) reverse transcriptase PCR (RT-PCR).[6] Real-time PCR involves the detection of a specific dye that stains non-covalently the target amplicon, which allows for quick results without much sample manipulation. Multiplex PCR simultaneously

detects several organisms by introducing different primer pairs to amplify DNA regions coding for specific genes of each bacterial strain targeted. Reverse-transcriptase PCR (RT-PCR) targets mRNA, which due to its rapid turnover and short half-lives in viable cells, can be used to determine if a bacterial cell is viable.[7] These relatively fast PCR techniques have a turnaround time of 5-24 hours due to the thermal cycling required in addition to other sample preparation steps; PCR schemes cannot meet the requirements demanded for near real-time reporting. Furthermore, these approaches can introduce ambiguities caused by the PCR process itself.[8-10]

FPGA Properties

Table S1. Comparison of conventional printed circuit board to an FPGA.

	Conventional Board	**FPGA**
Size (inches)	8 x 11	1 ½ x 1 ½
Speed (MHz)	20-50	200-500
Power Consumption	High	Low
Cost	High	Low ~$50

Microchip Fabrication

The microfluidic devices were replicated from a brass master (0.25” thick alloy 353 engravers brass, McMaster-Carr, Atlanta, GA) by high precision micromilling. Microstructures were milled onto the brass plate with a Kern MMP 2522 micromilling machine (KERN Micro-und Feinwerktechnik GmbH & Co., Germany). The mold master was heated to 160°C and pressed into the polymer, PMMA, with a pressure of 1,100 psi for 410 s using a PHI Precision Press (City of Industry, CA). The microfluidic channels were formed by annealing a cover slip (PMMA

sheet of 0.25 mm thickness) to the PMMA substrate. The chip was clamped between two glass plates with the assembly placed in a GC oven and the temperature raised to slightly above the T_g (107°C) of PMMA for 20 min.

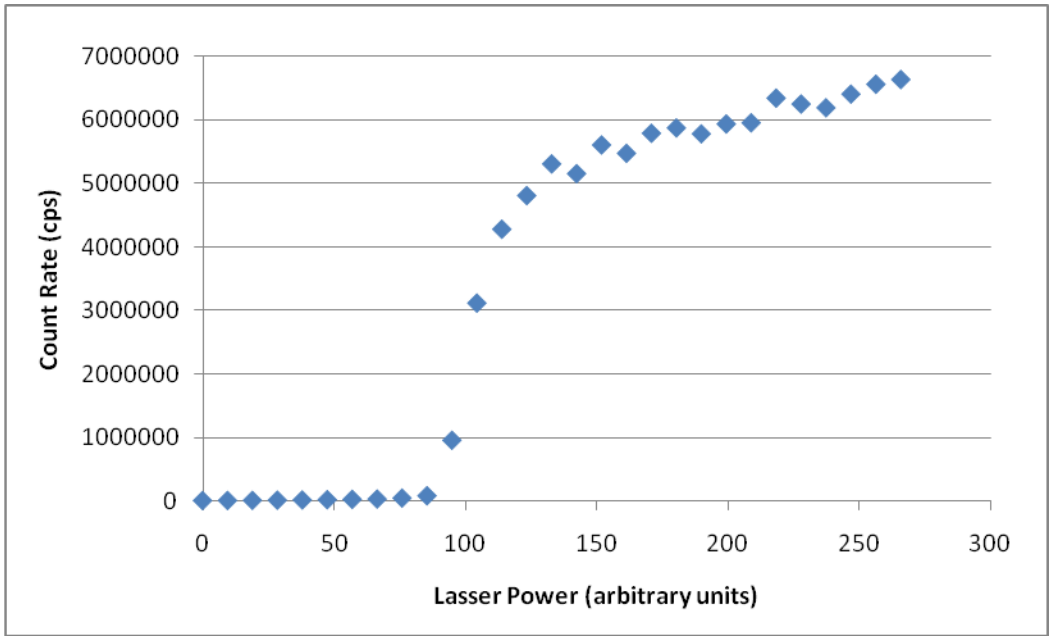

Figure S1. Graph showing the SPAD response to different fluorescent light levels altered by increasing the drive current to the VCSEL. The channel was filled with 0.1 mM of Alexa Fluor 660, which was continuously pumped (0.1 mL/h) through the detection zone and the laser power adjusted by increasing the drive current to the diode. The initial flat section in the plot is due to the drive current being below the lasing threshold (~110 mA). The detector saturates at a photon arrival rate of approximately 5M cps.

SPAD

The instantaneous photon flux from individual molecules producing photon bursts can be relatively high. Therefore, the saturation point of the SPAD used in these experiments was determined by filling the detection zone with Alexa Fluor 660 and adjusting the incident laser power, the results of which are shown in Figure S1. The lower plateau region resulted from the current level applied to the laser being below the lasing threshold and therefore, changes in the laser drive current produced no observable changes in the count rate. After the lasing threshold was reached, there was an increase in the counting rate. The upper plateau was reached at a count rate of 5 x 10^6 cps and resulted from detector saturation. The active quenching circuit

could not reset the SPAD before the next incident photon arrived at the photoactive area, producing non-linearity in the count rate with laser power.

Determination of the Sampling Efficiency (SE) and the Detection Efficiency (DE)

Table S2 shows the percent occupancy for each sample along with the delivery rate (DR), theoretical results in events/min, experimentally observed events/min and the calculated sampling efficiency (SE). These results were determined based on the data shown in Figures 6 and 7. The DR was calculated by multiplying the dye concentration by the flow rate (.01 mL/h or 1.7×10^{-7} L/min) and Avogadro's number. Based on the average illumination radius (25 μm and the channel cross section (120 μm x 120 μm), a SE of 13.6% was calculated. The theoretical results were obtained by multiplying the DR by the SE. The detection efficiency (DE) was determined by dividing the experimental results by the theoretical results. The average experimental DE was 22.6%. The relatively low DE is most likely due to; The sample passing through the probe volume but not counted as a true event due to the low numbers of photons it generated (false negative), or the inefficiency of hybridization of the MB at low concentrations, which would decrease the number of expected events.

Table S2. Summary of the run parameters and run conditions extracted from the calibration plot shown in Figure 7.

Sample	Concentration of DNA Target	Occupancy	Delivery Rate (events/min)	Theoretical Results* (events/min)	Actual Results (events/min)	Detection Efficiency
a)	5.00E-16	0.03	50	6.8	1.33	19.6
b)	1.00E-15	0.06	100	13.6	3.67	27.0
c)	5.00E-15	0.29	500	68	12.67	18.6
d)	1.00E-14	0.59	1000	136	34.33	25.2
*Based on a SE of 13.6% times the DR						

References

1. M. A. Northrup, B. Benett, D. Hadley, P. Landre, S. Lehew, J. Richards and P. Stratton, *Anal. Chem.*, 1998, **70**, 918-922.
2. B. S. Lee, J. N. Lee, J. M. Park, J. G. Lee, S. Kim, Y. K. Cho and C. Ko, *Lab Chip*, 2009, **9**, 1548-1555.
3. T. Zhang and H. H. P. Fang, *Appl. Microbiol. Biotechnol.*, 2006, **70**, 281-289.
4. N. Y. Fortin, A. Mulchandani and W. Chen, *Anal. Biochem.*, 2001, **289**, 281-288.
5. M. M. Shi, *Clinical Chemistry*, 2001, **47**, 164-172.
6. G. V. Kaigala, V. N. Hoang, A. Stickel, J. Lauzon, D. Manage, L. M. Pilarski and C. J. Backhouse, *Analyst*, 2008, **133**, 331-338.
7. G. E. C. Sheridan, C. I. Masters, J. A. Shallcross and B. M. Mackey, *Appl. Environ. Microbiol.*, 1998, **64**, 1313-1318.
8. J. Peccoud and C. Jacob, *Biophys. J.*, 1996, **71**, 101-108.
9. A. K. Bej, M. H. Mahbubani and R. M. Atlas, *Crit. Rev. Biochem. Mol. Biol.*, 1991, **26**, 301-334.
10. J. Reiss, M. Krawczak, M. Schloesser, M. Wagner and D. N. Cooper, *Nucleic Acids Res.*, 1990, **18**, 973-978.